NICOP Project Report

DISTRIBUTION STATEMENT A. Approved for public release; distribution is unlimited.

Cross-slope Acoustic Scattering and Transmission Experiment (CASTEx) in the Northeastern South China Sea

Dr. Yung-Sheng Chiu
Institute of Undersea Technology, National Sun Yat-sen University
No. 70, Lienhai Rd., Kaohsiung, 80424, Taiwan, R.O.C.
phone: (886) 7-5255287 fax: (886) 7-5255288 email: linusyschiu@gmail.com

Award Number: N62909-19-1-2070

BACKGROUND

Sound transmission in the sloping environment of the South China Sea (SCS) shows inherent spatial and temporal instabilities or fluctuations that can be attributed to environmental factors. From 2001 to 2015, a series of joint Taiwanese–U.S. field experiments were conducted in the SCS, for example ASIAEX, VNAS/WISE, and SCOPE/NLIWI; further, sand dune acoustic experiments were also conducted to survey the regional oceanic variabilities and the temporal and spatial variabilities in acoustic propagation in the SCS. The synthesis of the acoustic results obtained through experimentation provides information on the nature of dependency of signal fluctuations on the locale, orientation, range, and strength of nonlinear internal waves (NIWs); the acoustic results also provide insights into the subaqueous sand waves. However, the combined effects of NIWs, sand waves, and topographic variation are still unknown. Further, the potential impact on long-range cross-slope acoustic transmission, with respect to both phenomenology and statistics, is also not clearly understood. To address these issues, we focus on the existing problems on acoustic variations in the northeastern (NE) SCS, from the upper slope, through areas with bedforms and shelf break, and to the shelf regime. Subsequently, the areas are accessed contrariwise as well.

OBJECTIVES

The objectives of the proposed research for FY19–21 are two-fold:

1. To continue and complete the synthesis of the acoustic results from four transmission experiments: ASIAEX, VANS/WISE, NLIWI, and the sand dune acoustic experiment. These experiments were conducted in the vicinity of the NE SCS shelf break and upper slope to investigate the dependence of signal fluctuations on the locale, orientation, range, and the type and strength of NIWs and sand dunes.
2. In collaboration with the US scientist, Dr. Ying-Tsong Lin of the Woods Hole Oceanographic Institution (WHOI), we jointly planned and executed the field study consisting of the analysis of systematic and concurrent acoustic propagation, bottom/sub-bottom profiling, and oceanographic measurement to investigate the combined environmental effects on sound transmission in the upper slope, shelf break, and shelf of the NE SCS. Particularly, the joint field study has the following overall scientific objectives:

- Long-range propagation from the basin, deep into the shelf, and contrariwise: We measure the distance sound can propagate into an area exhibiting such a geometry and gain insights into the roles that acoustic scattering, stripping, and attenuation processes play in limiting the sound propagation range as sound traverses the three geographical regimes.
- Three-dimensional (3D) propagation effects: (1) Investigation of horizontal refraction, reflection, and/or diffraction of the sound propagating across the slope (along isobath lines); (2) Consideration of bathymetric interaction with the sloping bottom and/or sand waves; and (3) Collection of evidence to support the existence of the three types of horizontal modes: whispering gallery, full bouncing, and leaky modes, predicted for the curved internal wave ducts based on theory.
- Geoacoustics: Investigation of the spatial variability of the geoacoustic parameters on the shelf, shelfbreak, and slope as well as on the different provinces in each of the three aforementioned geographical regimes. The geoacoustic parameters is estimated based on two methods: the normal incidence chirp sonar (survey) method and the wide-angle reflection coefficient (spot measurements) method.

APPROACH

All field work proposed here has been conducted in collaboration and coordination with the US colleagues from WHOI, and the Taiwan Research vessels (RVs): OR1, OR2, OR3, and Legend have been utilized. Under the sponsorship of the Taiwan Ministry of Science and Technology (MOST), the cross-slope Acoustic Scattering and Transmission Experiment (CASTEx) was planned to be conducted in 2019–2021. The pilot acoustic experiment was performed in May 2019, and the intensive main experiment was conducted in October 2020.

To collect bathymetric data and coring data from the experimental area, one five-day cruise each year with the RV Legend, was planned to conduct the multibeam bathymetric survey (MEBS) and surficial sediment coring. The designated survey area for each year is shown in Figure 1. Three 10 km × 24 km areas, spanning the upper slope, shelf break, and shelf, were chosen for FY19, FY20, and FY21, respectively. For each year, the RV Legend has been dedicated to performing an MBES, collecting sediment core samples, and deploying CTD to monitor water column variations. The hull-mounted multibeam system of the RV Legend provides high-quality bathymetric mapping across the slope, whereas its dynamic positioning (DP) system is ideal for use in sediment coring and CTD deployment.

For the acoustic transmission study, a pilot experiment and an intensive main experiment were planned for FY19 and FY20, respectively. For the pilot experiment in May 2019, three five-day cruises were planned, with RVs OR1 and OR3, operating together to obtain the necessary experimental design information. A small acoustic propagation experiment was conducted during the pilot experiment to obtain the initial observations of the long-range sound transmission effects. The 10 d mainly spanned a spring tidal cycle; during this cycle, the trans-basin NIWs are generally expected to have maximum amplitude and amplitude variations. During the 10 d, the RV OR1 was used to deploy and recover moorings, follow nonlinear internal waves, and measure their physical characteristics in situ using a lowered package of oceanographic sensors. RV OR3 operates a mid- and low-frequency towed source and a receiver array across and along the slope to collect acoustic transmission data and geoacoustic

data. Multiship operations facilitate obtaining longer and more complete acoustic data by utilizing the limited acoustic systems.

For the small acoustic transmission experiment in FY19, one midfrequency (3–7 kHz) source mooring from NSYSU, two four-channel receiver array moorings from NSYSU and NTU, and one four-channel receiver array mooring from WHOI was deployed across the slope of NE SCS. Based on the predefined plan, the moored source/receiving systems were deployed separately on the shelf and upper slope, and the towed source/receiving systems from NSYSU were deployed and towed between the moored systems to monitor the acoustic signals and perform the geoacoustic survey. For oceanographic monitoring, one of the moorings, instrumented by our colleagues from Taiwan, was equipped with high-resolution pressure, current, and turbidity sensors to characterize the sediment resuspension process and capture the associated intracycle time and space scales.

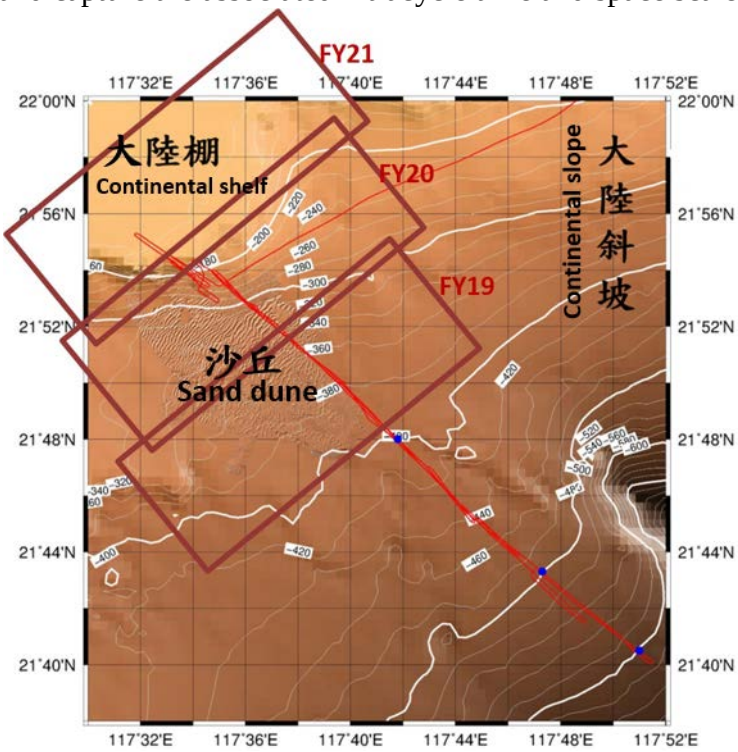

Figure 1 Three MBES survey areas for FY19, FY20, and FY21.

For the intensive main experiments in FY20, four five-day cruises with RVs OR1 and OR3, operating together, were planned. The cruises overlapped, and, therefore, they spanned a complete spring and neap tidal cycle; generally, during this cycle the NIWs are expected to have the maximum and minimum amplitudes. For the acoustic transmission experiment in FY20, one midfrequency and one low-frequency source moorings from NSYSU and four four-channel receiver array moorings from NSYSU and NTU were deployed across the slope. Additionally, two low-frequency source moorings and five four-channel receiver array moorings from WHOI were deployed along the slope to measure acoustic horizontal refraction effects. During the experiment, RV OR1 was used to deploy and recover moorings, follow nonlinear internal waves, and measure their physical characteristics in situ using the lowered package of oceanographic sensors. RV OR3 operated the mid- and low-frequency towed source and a receiver array across and along the slope to collect acoustic transmission data and geoacoustic data.

Data analysis commenced immediately after the pilot experiment and intensive main experiment; the data analysis will be continued until the end of FY21. This entails time series analysis and modeling to characterize and elucidate the two-dimensional (2D) long-range and 3D phenomena in the measured sound field as well as the geoacoustic parameters and the associated ocean dynamics. The focus of the analysis is to investigate the relationship between the observed characteristics and statistics of the 2D and 3D acoustic field, and the observed characteristics of the NIWs, sand dunes, and slope. The research activities for FY19–FY21 are summarized in the table below.

Table 1 Research plan for FY19–FY21

	FY19	FY20	FY21
MBES survey	upper slope	shelf break	shelf
Sediment coring	upper slope	shelf break	shelf
Geoacoustic survey	cross slope	cross slope	cross slope
Acoustic transmission exp.	cross slope (pilot experiment), data analysis	cross slope (intensive main experiment), data analysis	data analysis
Oceanographic observation	pilot experiment, data analysis	Intensive main experiment, data analysis	data analysis

WORK COMPLETED UNTIL NOW

In 2019 and 2020, the pilot experiment and the intensive main experiment, respectively, were conducted. In both the years, multibeam surveys and acoustic experiments were conducted. The research cruises and the corresponding works completed are listed in Table 2. The details of the pilot experiment and the intensive main experiment are summrized as follows.

Table 2 Research cruises and works completed in 2019 and 2020

2019- Pilot Experiment			
1	RV OR 3	2019/5/11-5/15	2D/3D acoustic propagation experiment
2	RV OR 1	2019/5/13-5/18	mooring recovery
3	RV OR 3	2019/5/28-6/01	core sample collection, geoacoustic survey
2020- Intensive Main Experiment			
1	RV OR3	2020/9/15-9/18	multibeam survey
2	RV Legend	2020/10/14-10/19	2D/3D acoustic propagation experiment, geoacoustic survey, multibeam survey

1. Pilot Experiment

A pilot experiment was conducted in the NE SCS in May 2019, in which Dr. Ying-Tsong Lin and the WHOI technician, Peter Koski, participated. For the experiment, three legs of the cruise of RVs

OR1 and OR3 were involved, and a total of five moorings of acoustic and oceanographic gears were deployed. The designed experimental area and mooring sites are shown in Figure 2; the sites M-380, M-200, and M-120 correspond to the slope, shelf break and shelf, respectively. Using WHOI gears, the M-120 site was slightly modified, and the M-WHOI site was designed at the edge of the shelf, as shown in Figure 3.

For acoustic transmission experiments, towed and moored sources from NSYSU and WHOI were deployed to transmit midfrequency and low-frequency signals along a designed 20 km track. Figure 4(a) shows the towed vehicle with midfrequency and low-frequency sources from NSYSU. These signals were received by the moored and towed receivers; the data collected indicate a high SNR and a low-frequency signal propagated over 20 km. Figure 4(b) illustrates the acoustic propagation from towed sources to the NSYSU receiver at M-120. For the collection of oceanographic data, an ADCP from NTU was deployed and multiple T/P sensors were mounted onto the moorings to monitor the temperature profiles. In addition, a chirp sonar survey was conducted to collect geoacoustic data. Figure 4(c) shows the pictures of the deployment of the source and receiver system.

1.1. Ship Time and MBES Survey

Using the funding provided by the FY19 budget of the NICOP project, two days of RV Legend ship time was purchased. Further, participation in the experiment in 2020 was also planned. Furthermore, a set of Multibeam survey data in the sand dune area of the SCS was purchased from TORI.

1.2. Acoustic Simulation and Data Analysis

A post-doctoral fellow, Dr. Yuan-Ying Chang, participated in this project and worked on acoustic modeling and data analysis. The experimental data were preliminarily analyzed, and the acoustic arrival patterns were obtained.

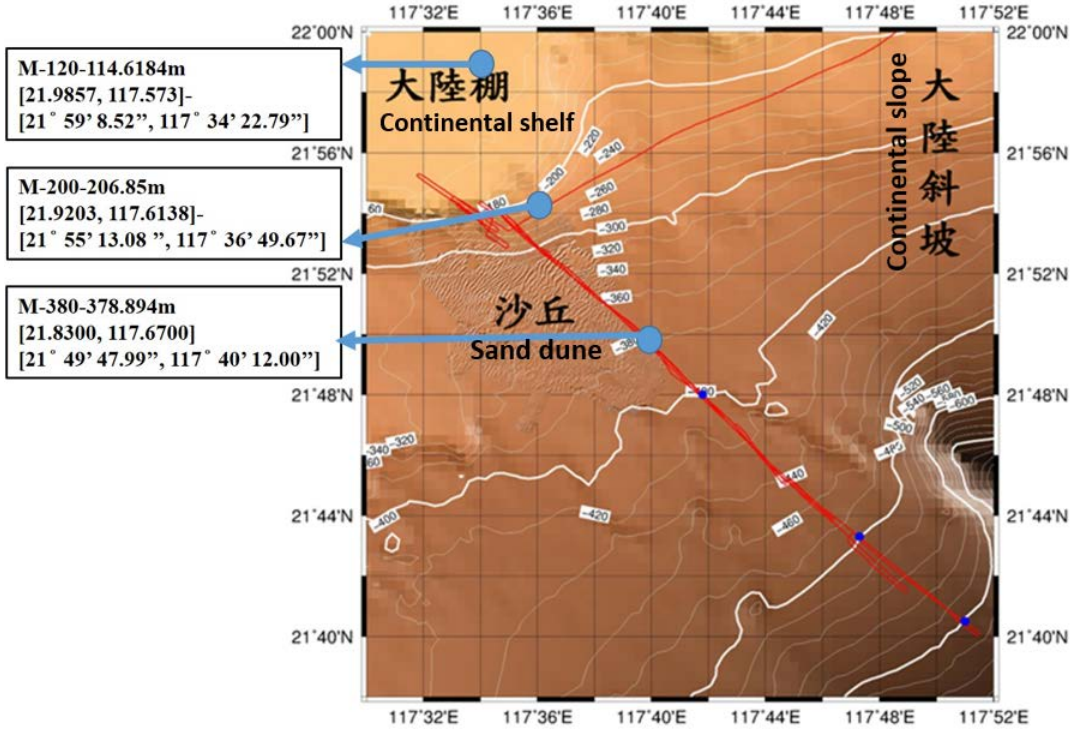

Figure 2 Designated experimental area and mooring sites.

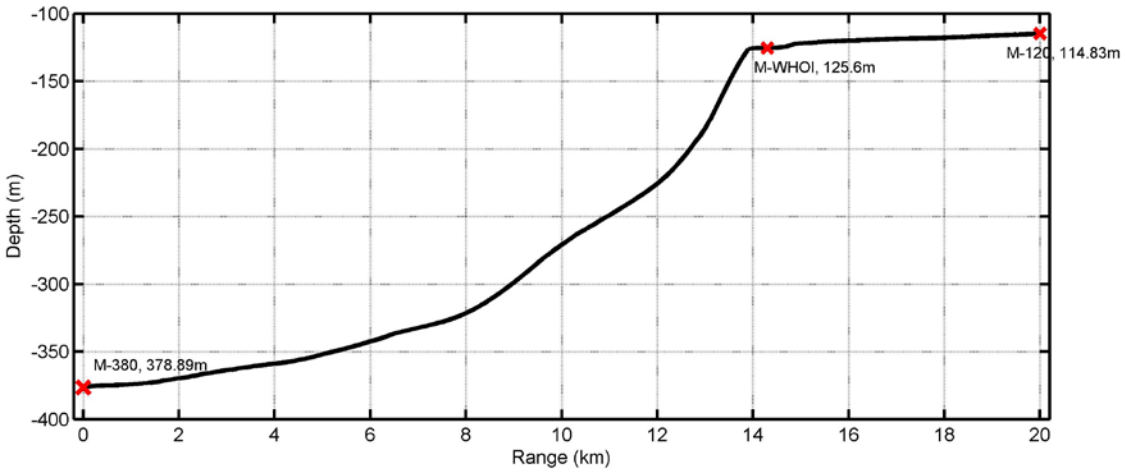

Figure 3 Main acoustic mooring sites.

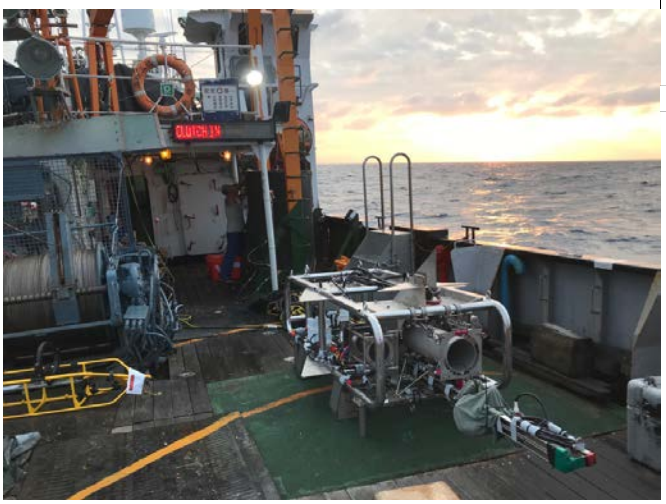

(a)

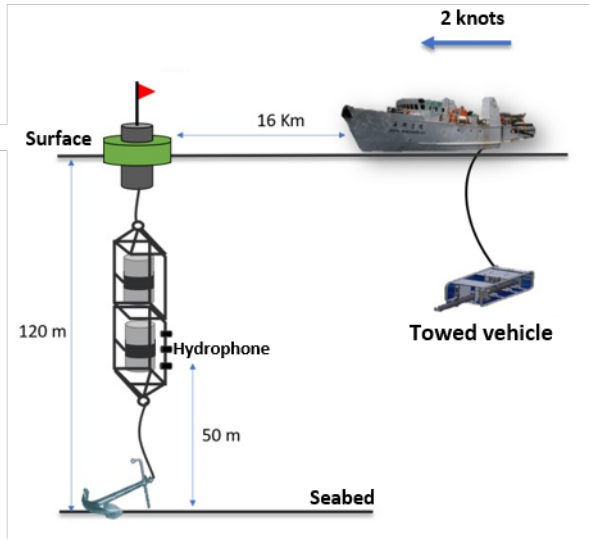

(b)

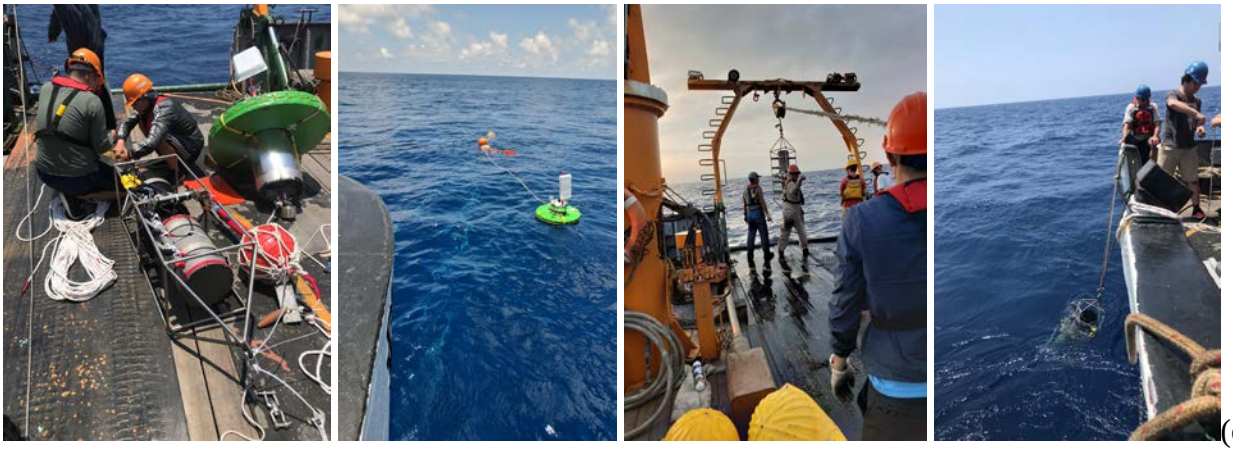

(c)

Figure 4 (a) Towed vehicle with midfrequency and low-frequency sources from NSYSU. (b) Illustration of the acoustic propagation from towed sources to the NSYSU receiver at the M-120 site. (c) Pictures of the deployments.

1.3. Acoustic Propagation Data Results

Eight repeated towed acoustic tracks across the slope were conducted in the pilot experiment, as shown in Figure 5, including four long tracks and four short tracks. During the towing, midfrequency (3–7 kHz) and low-frequency (600–1000 Hz) signals were transmitted and recorded by the receivers at M-120, M-200, and M-380. Figure 6–13 show all the eight sets of the midfrequency acoustic propagation data; temporal variations can be clearly observed in the arrival patterns and received energy. The M-120 site is approximately 6 km from the shelf break. In most of the dataset, the shelf break was found to have hindered the acoustic propagation toward the shelf, and the received energy indicated obvious decay while the source-receiver range is larger than 6-8 km. This effect can also be seen in the modeled TL in Figure 14. Some tracks show that the midfrequency signal can propagate over 12 km and be received by the receiver at M-120; as an example, the received signal of track 2–9 is illustrated in Figure 12. This variation can indeed be attributed to the watercolumn variations. The temperature and depth data monitored at the M-120 site is shown in Figure 22; the red curves mark the

time period for track 2–9 and indicate an internal wave package that has passed along the acoustic propagating path. Moreover, the variations manifested both in the received energy and as the scattering effect. More diversed and distincted arrivals are observed in tracks 2–8 and 2–9 compared with the other tracks. The modeling works will be studied further to confirm the effects of the internal waves on the acoustic propagation in this area.

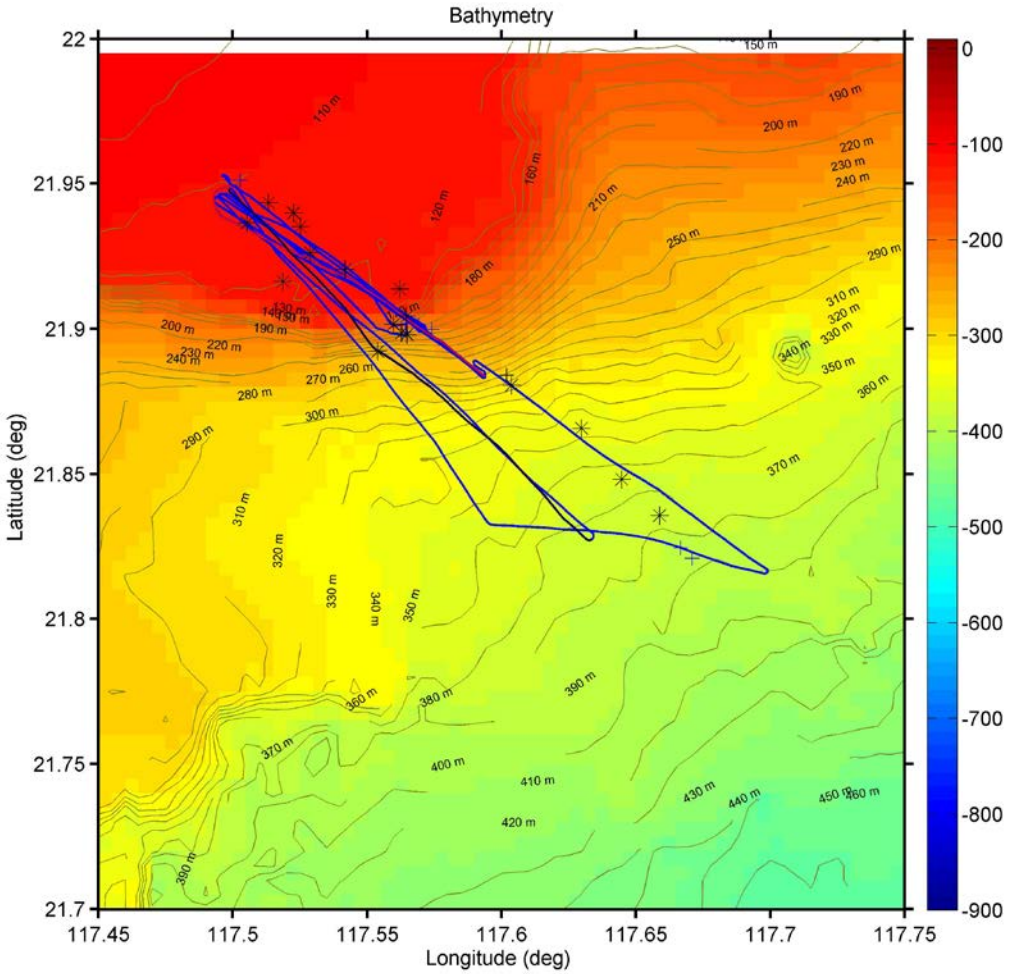

Figure 5 RV OR3 towing tracks during acoustic propagation experiment.

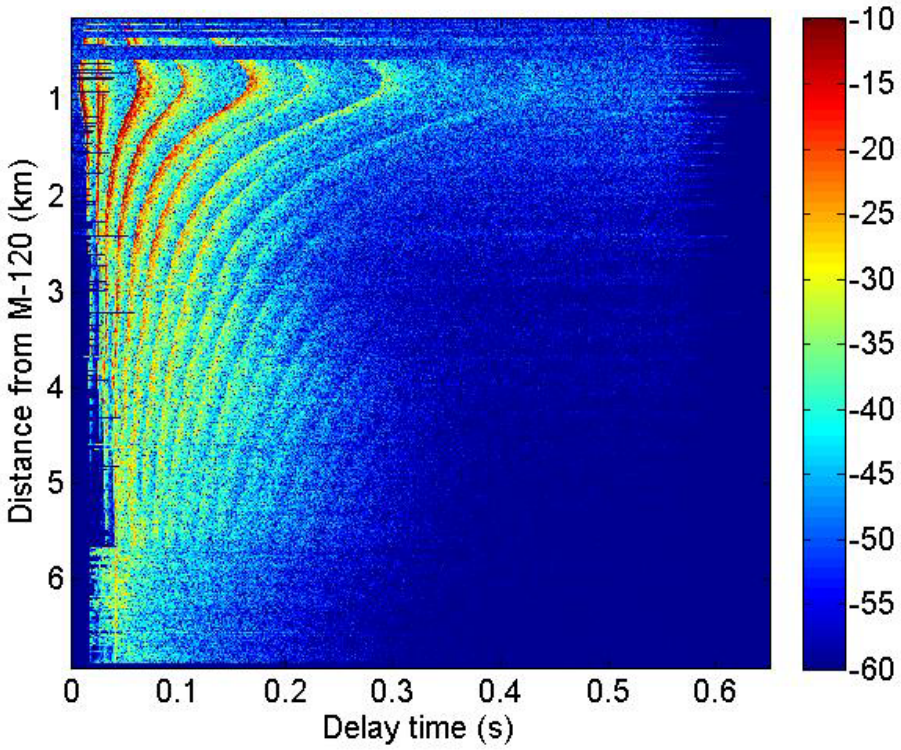

Figure 6 Track 1 of the midfrequency (3–7 kHz) acoustic propagation data.

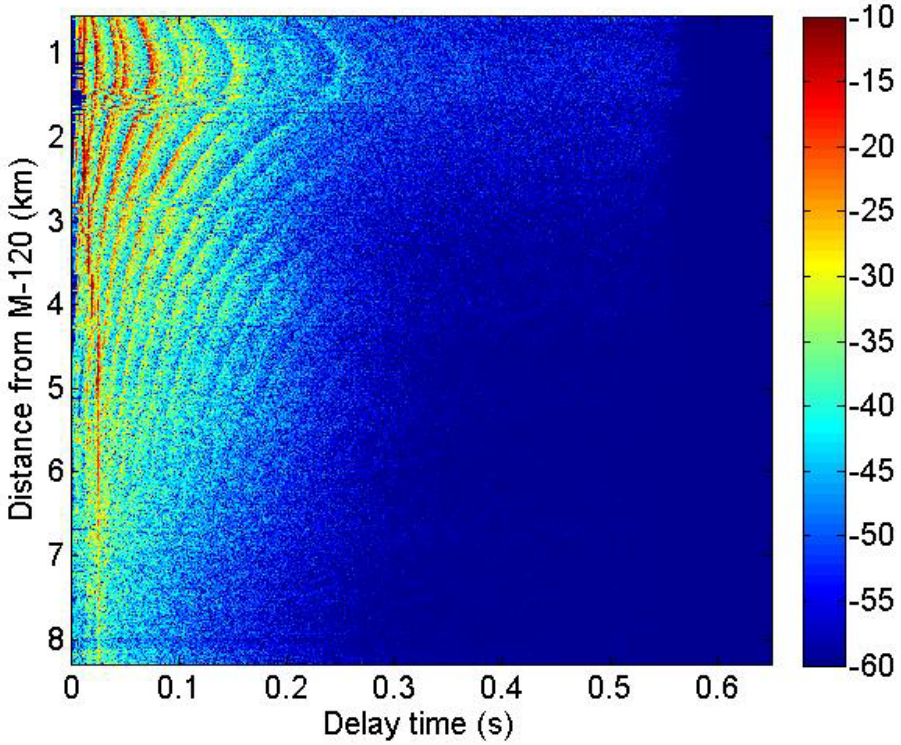

Figure 7 Track 2–3 of the midfrequency (3–7 kHz) acoustic propagation data.

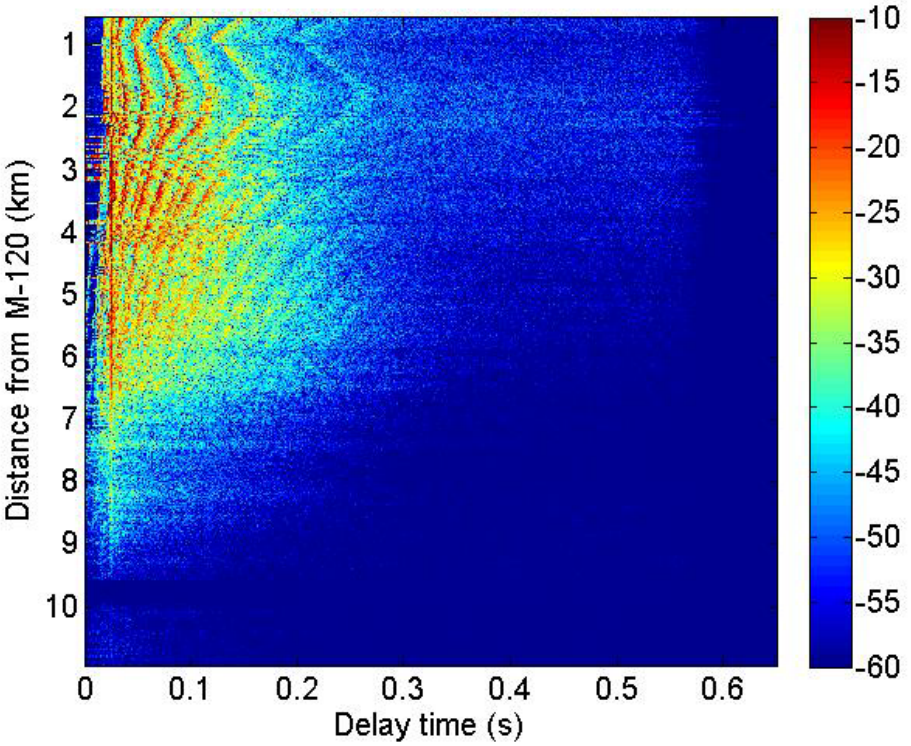

Figure 8 Track 2–4 of the midfrequency (3–7 kHz) acoustic propagation data.

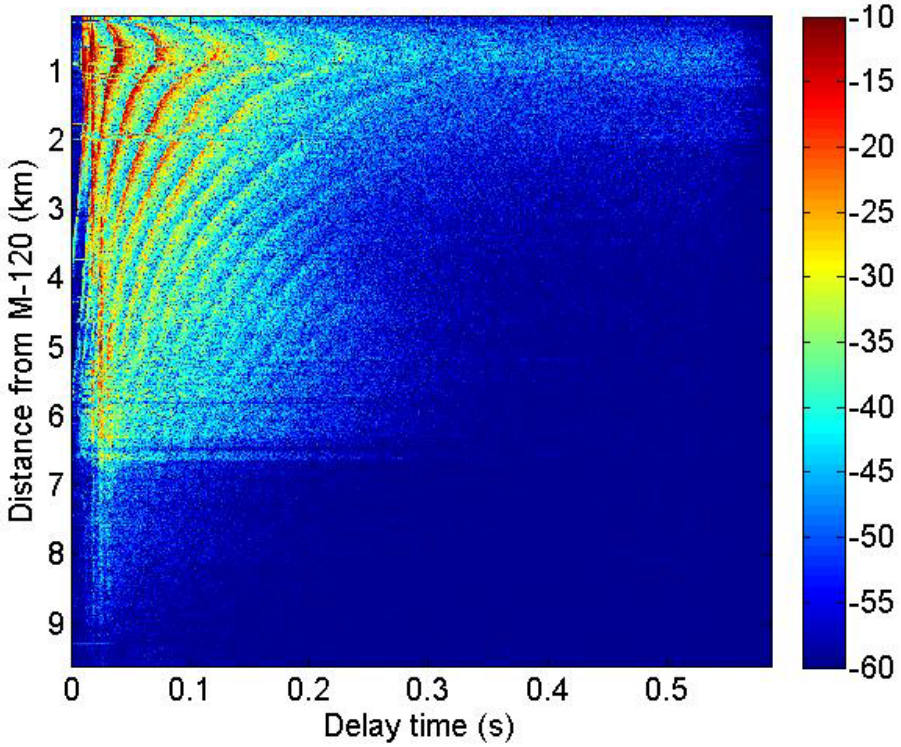

Figure 9 Track 2–5 of the midfrequency (3–7 kHz) acoustic propagation data.

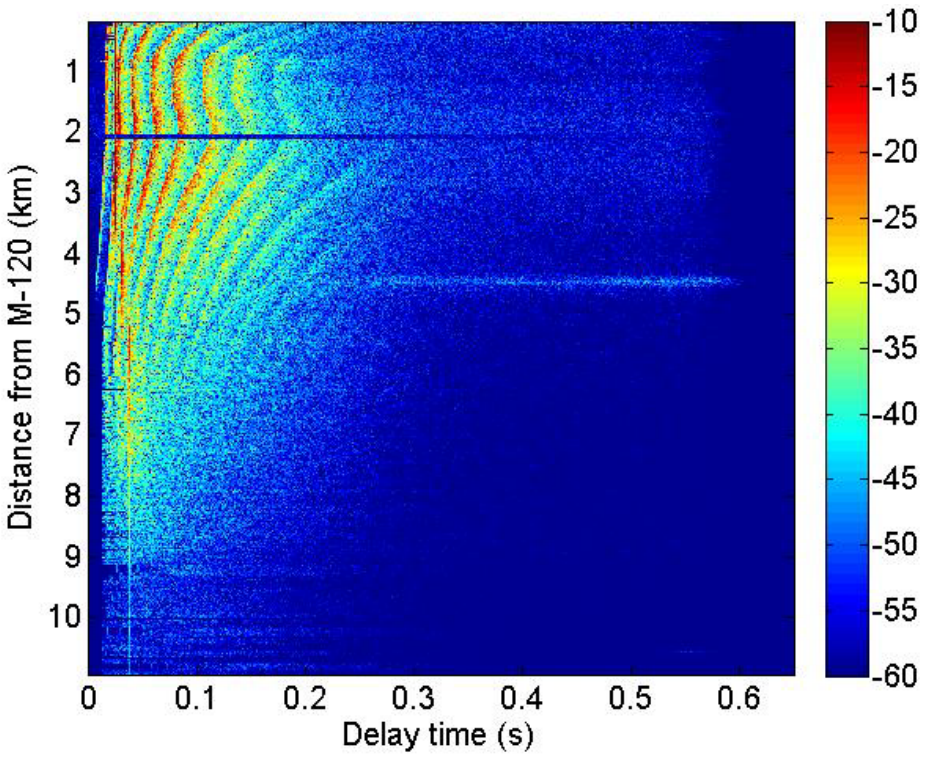

Figure 10 Track 2–6 of the midfrequency (3–7 kHz) acoustic propagation data.

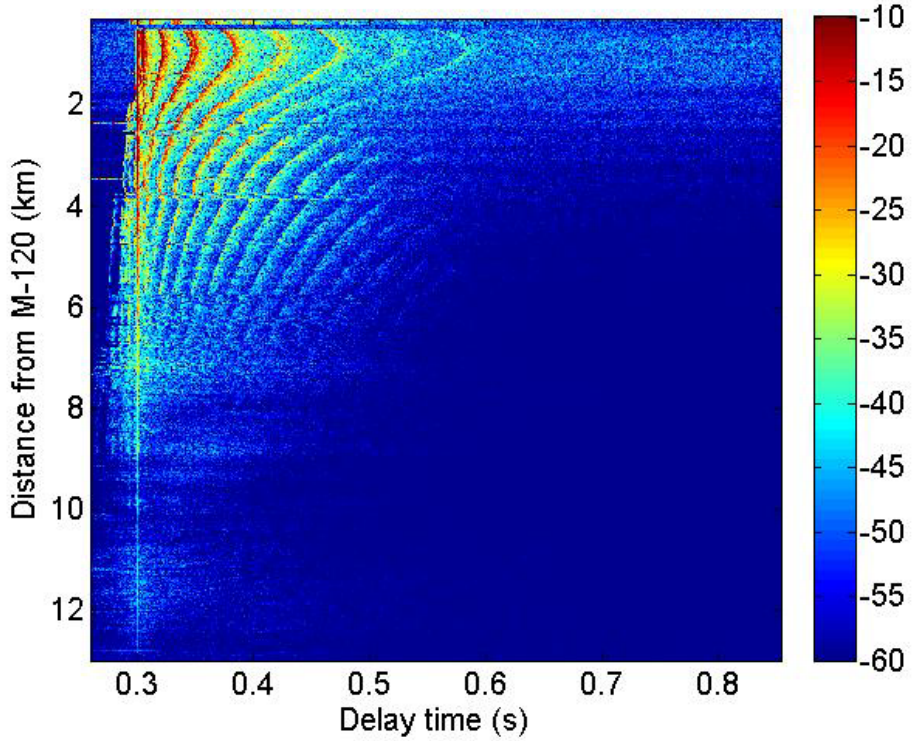

Figure 11 Track 2–8 of the midfrequency (3–7 kHz) acoustic propagation data.

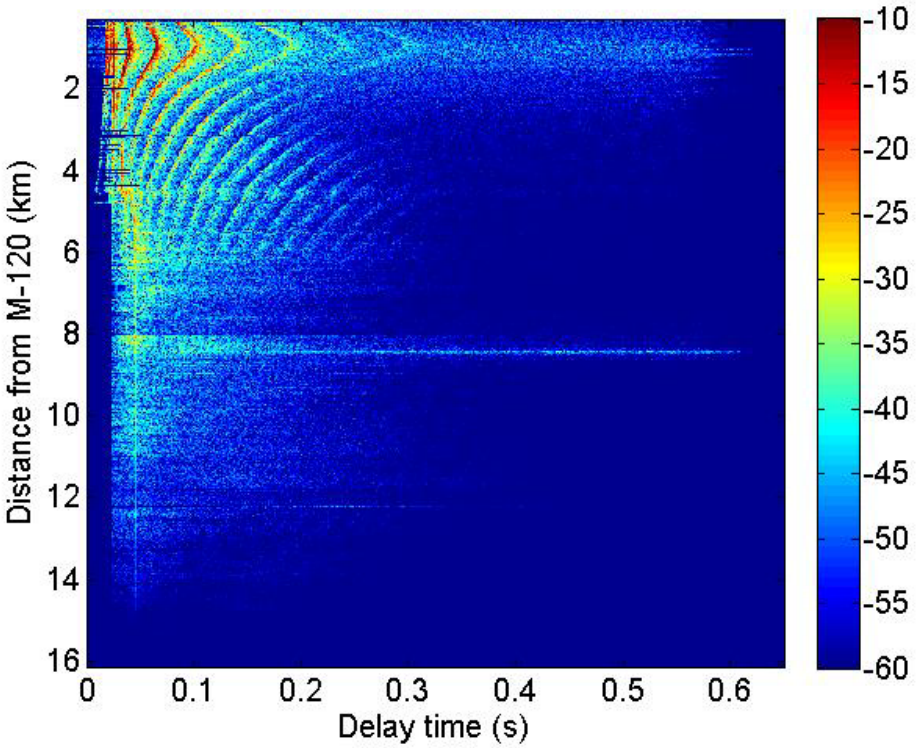

Figure 12 Track 2–9 of the midfrequency (3–7 kHz) acoustic propagation data.

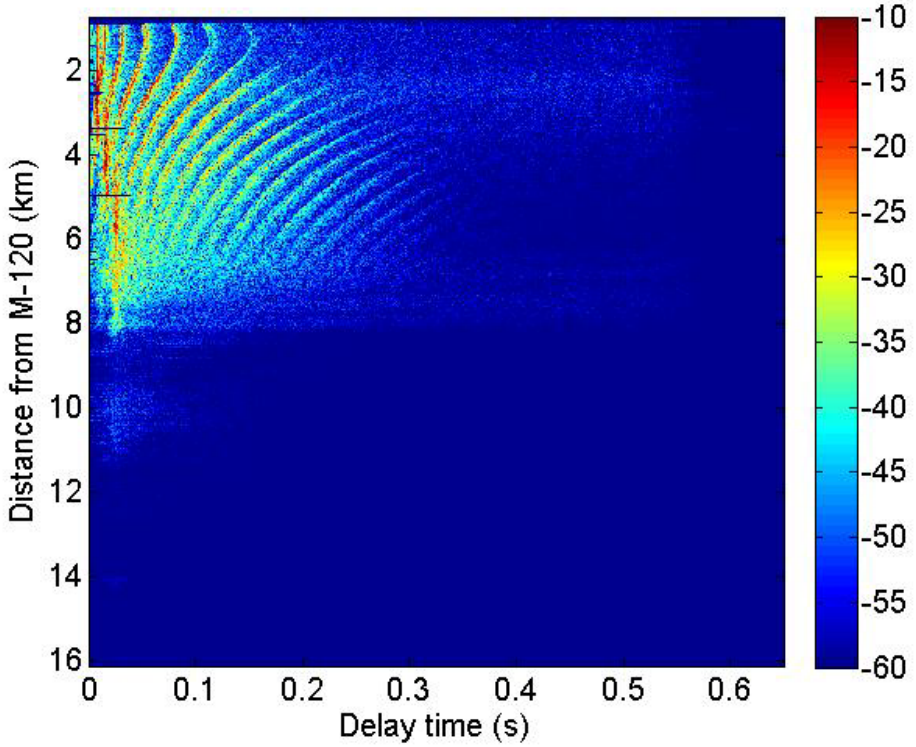

Figure 13 Track 2–10 of the midfrequency (3–7 kHz) acoustic propagation data.

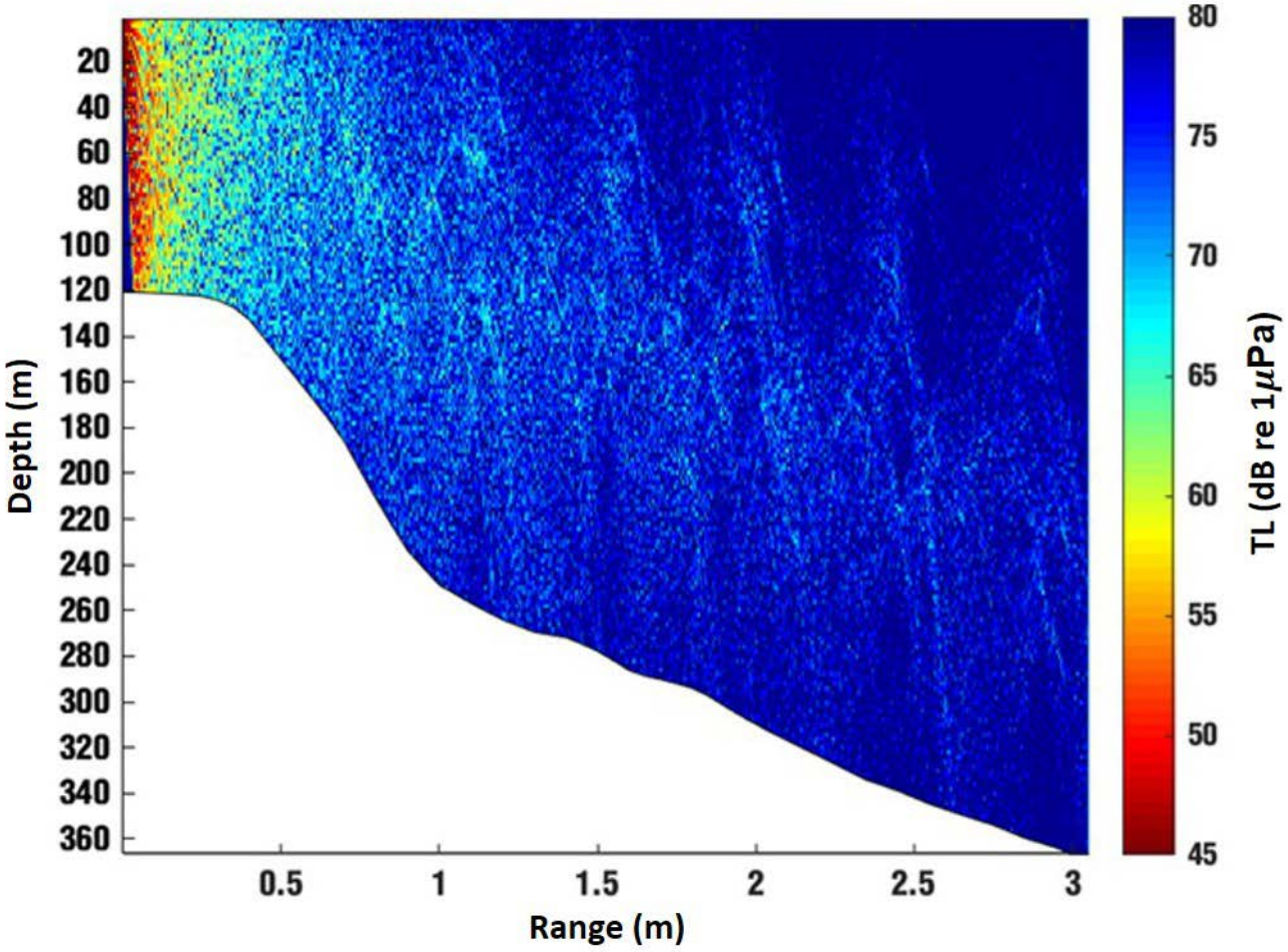

Figure 14 Experimental site transmission loss model.

Figure 15 shows the received arrival patterns of the low-frequency signal transmitted at different locations of track 2–8, corresponding to the locations 1–6 shown in the lowest panel in Figure 15. A high SNR was observed over the entire transect. Because the low-frequency trasmission was scheduled at the 0^{th} and 30^{th} min in each hour, transmitting a 15 min signal continuously, the low-frequency data did not cover the entire track. In the six transmissions shown in Figure 15, the received energy and arrival patterns show high spatial variations. The subaqueous sand dune bedforms mainly appear between location 3 and 4; therefore, the received signals corresponding to location 3 is more scattered.

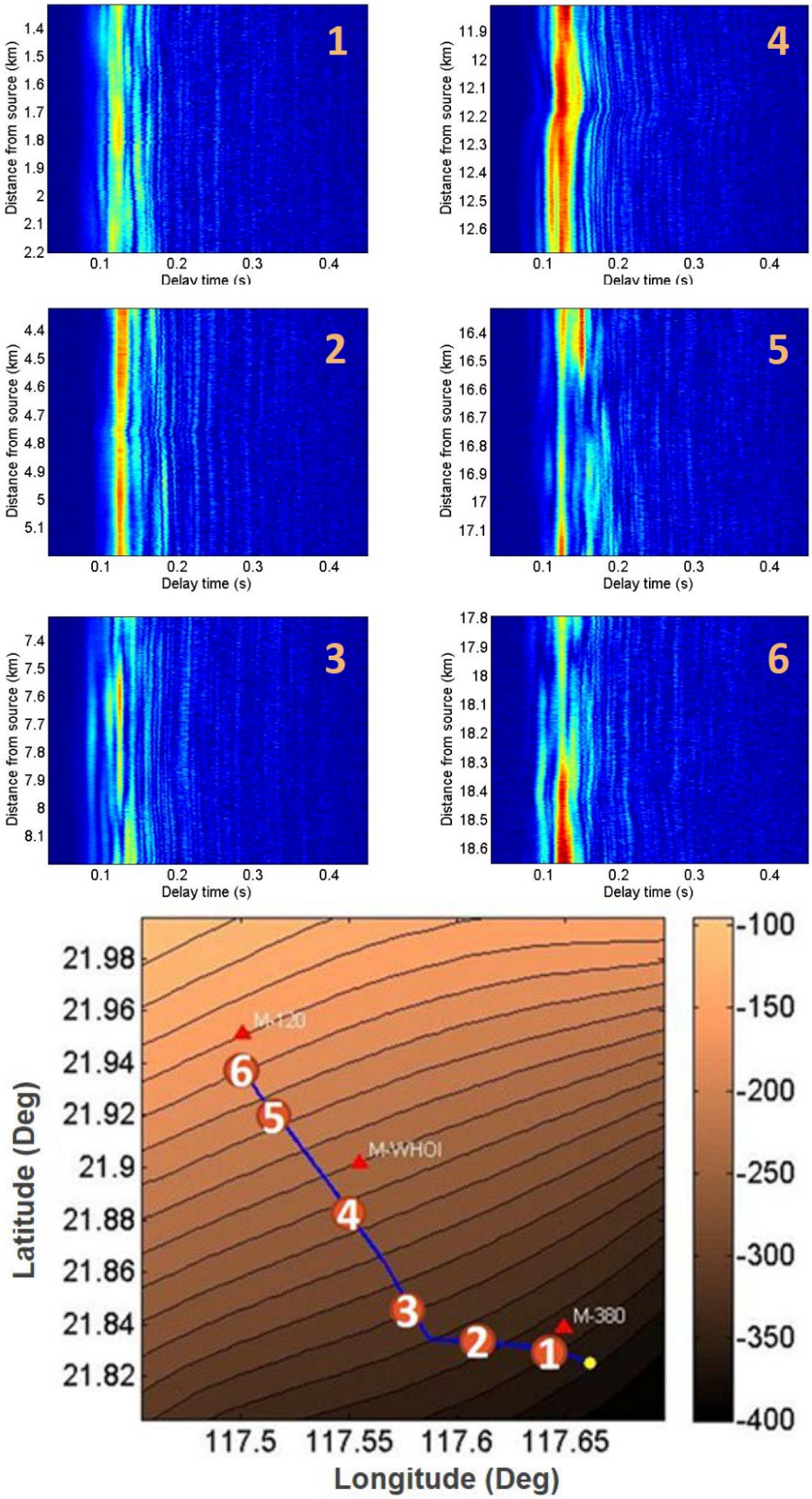

Figure 15 Received arrival patterns of the low-frequency signal transmitted at different locations.

1.4. Geoacoustic Survey Results

Two sub-bottom profiling survey transects were conducted in the pilot experiment. Figure 16 shows the echogram of one survey transect. Additionally, sediment samples were collected, as shown in Figure 17. All core samples were analyzed and the porosity, density, and mean grain size were obtained, as listed in Table 3. The normal incidence reflection data is used for geoacoustic inversion, incoporating the measured porosity and mean grain size. The effective density fluid approximation of the Biot model is applied for the geoacoustic inversion, and the sound speed, effective density, and attenuation of the surficial sediment layer are obtained. Figure 18 shows some of the core sample locations and the corresponding sound speed estimates. A lower sound speed is observed on the shelf break and slope, whereas a higher sound speed is observed on the shelf.

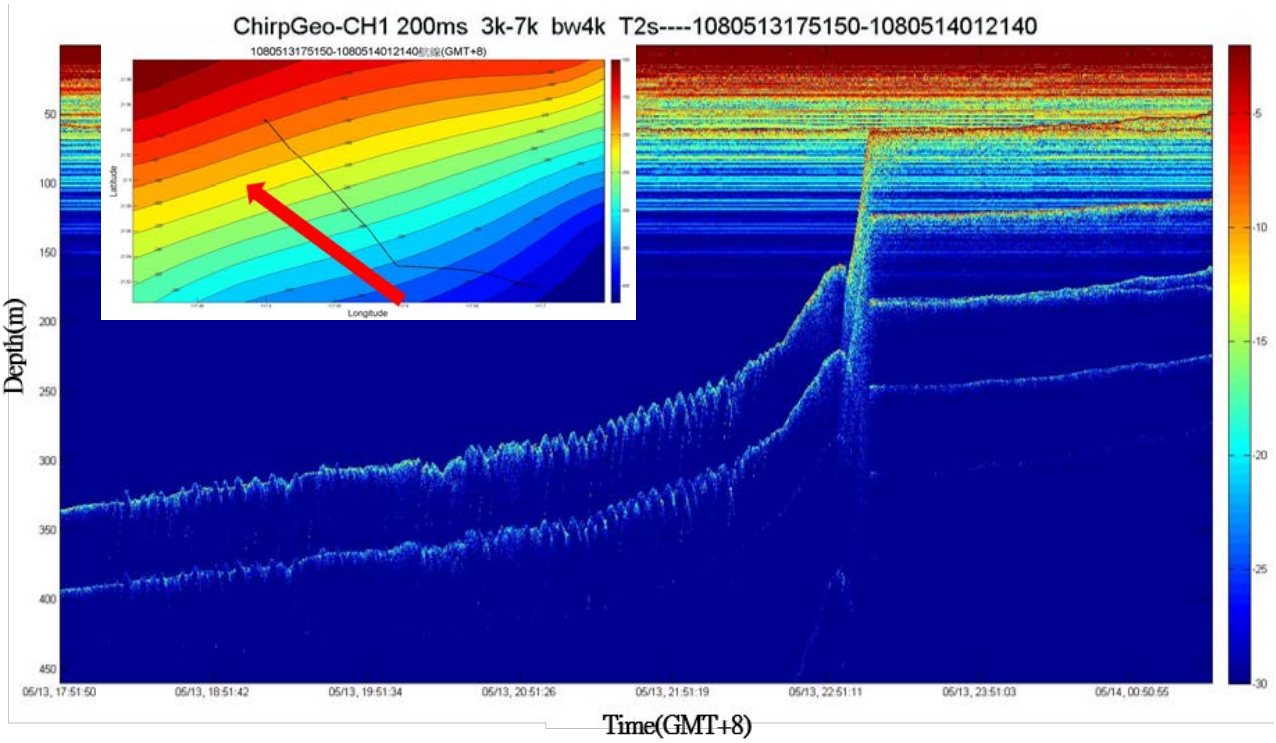

Figure 16 Echogram of a sub-bottom profiling survey transect.

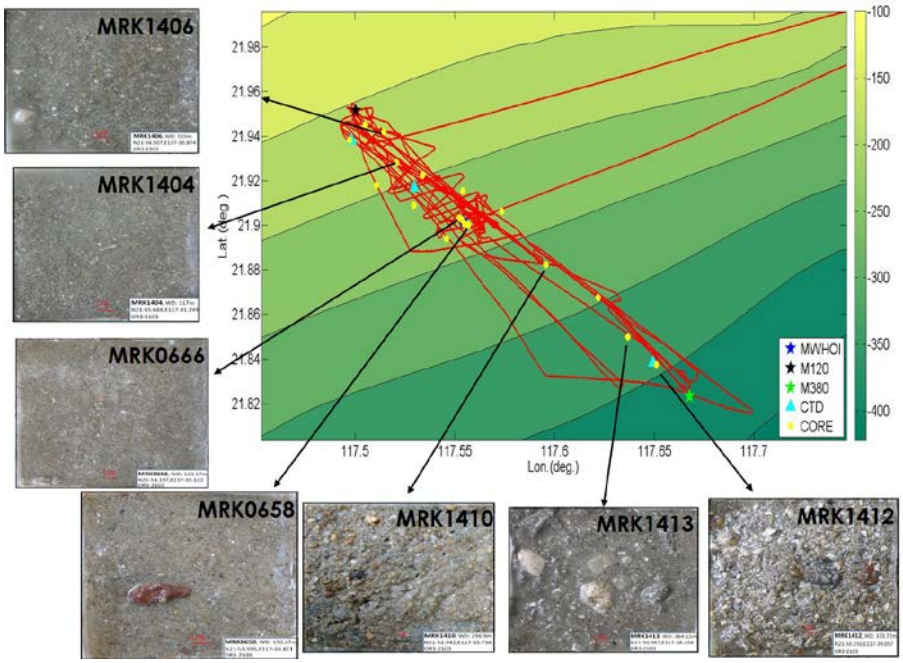

Figure 17 Collected sediment samples and the corresponding collecting sites.

Table 3 Locations and measured parameters of the core samples collected in 2019

Site	Longitude	Latitude	Porosity (%)	Density (g/cm^3)	Grain Size (μm)	Depth (m)
MRK0657	117.5628404	21.89853	0.29	2.18	380.4	144
MRK0658	117.5648	21.89796	0.27	2.21	545.5	150
MRK0666	117.5598809	21.90149	0.41	1.98	258.4	124
MRK0667	117.56475	21.9043	0.38	2.02	248.3	124
MRK0668	117.5621512	21.91364	0.45	1.91	321.1	121
MRK0669	117.5251893	21.93504	0.32	2.12	280.5	120
MRK1401	117.541857	21.92037	0.34	2.09	364.5	118
MRK1404	117.5288807	21.92614	0.29	2.18	493	117
MRK1405	117.5187029	21.91627	0.29	2.18	501.5	119
MRK1406	117.5226542	21.93986	0.25	2.24	490.7	115
MRK1407	117.513294	21.9433	0.29	2.17	401.1	113
MRK1408	117.5054025	21.93652	0.19	2.34	610	113
MRK1409	117.5539557	21.89215	0.45	1.90	63.39	235
MRK1410	117.6037624	21.88049	0.28	2.19	747.5	297
MRK1411	117.6297222	21.8657	0.42	1.95	18.43	343
MRK1412	117.6587442	21.83565	0.42	1.95	687.5	374
MRK1413	117.64466	21.84808	0.37	2.04	304	365

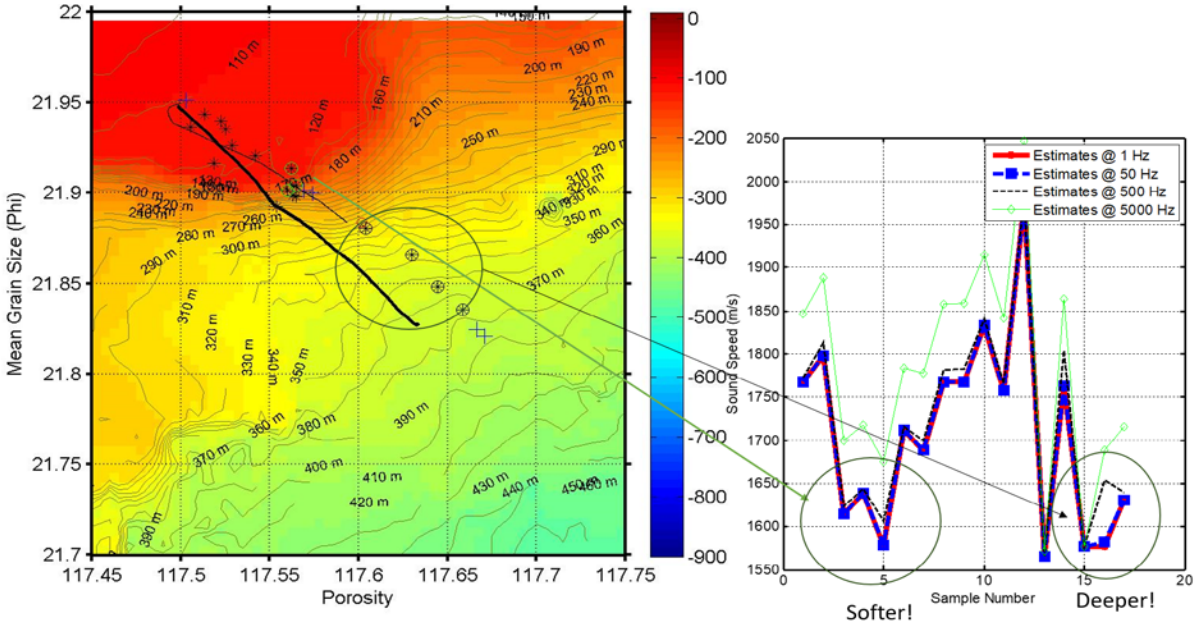

Figure 18 Core sampling locations and the corresponding inverted sound speed.

1.5. Multibeam Echo Sounding Survey Results

In the FY19 project, MBES data for the sand dune area, collected by the RV Legend, were obtained, as shown in Figure 19.

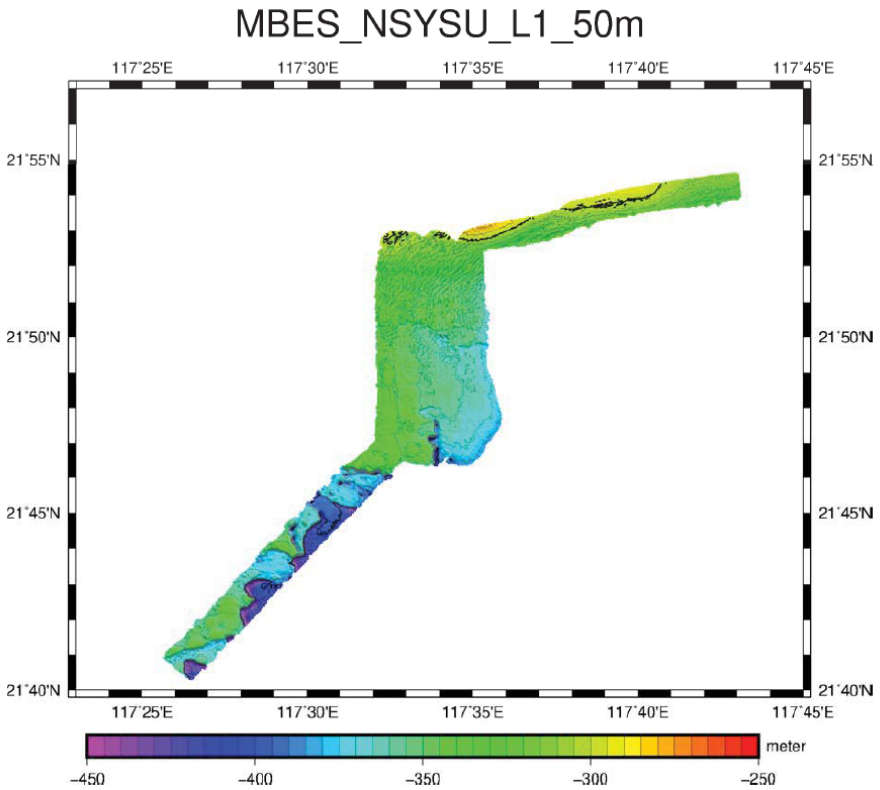

Figure 19 Multibeam echo sounding survey area and obtained data for the sand dune area collected by the RV Legend.

1.6. Oceanographic Data Results

The CTD data of three mooring sites were collected, as shown in Figure 20. Figure 21 shows the result of the sound speed profile from three sites. The M-120 moorings were mounted with five T/P sensors and the corresponding result is shown in Figure 22.

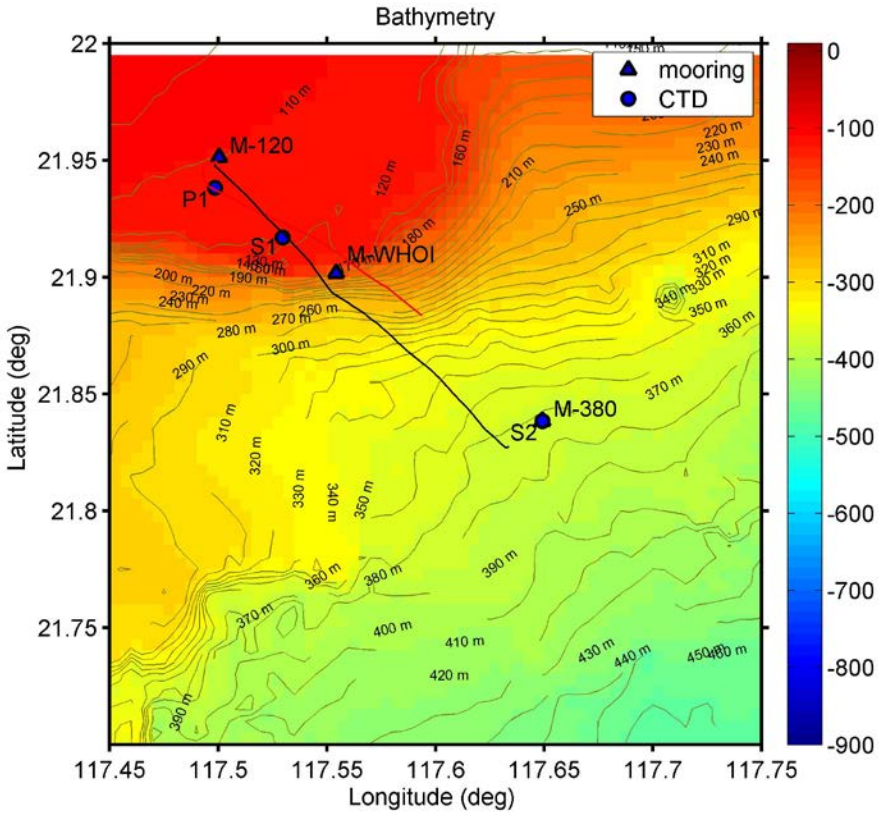

Figure 20 Ship Time and Multibeam Echo Sounding Survey.

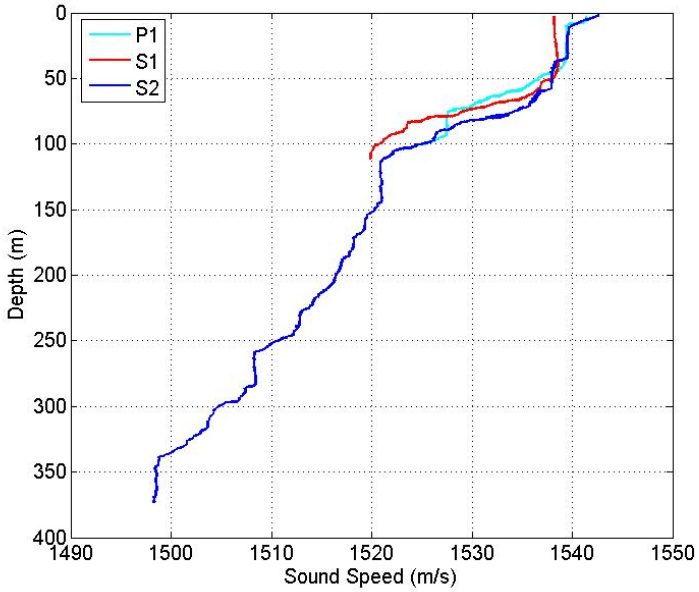

Figure 21 Sound speed profile of three mooring sites.

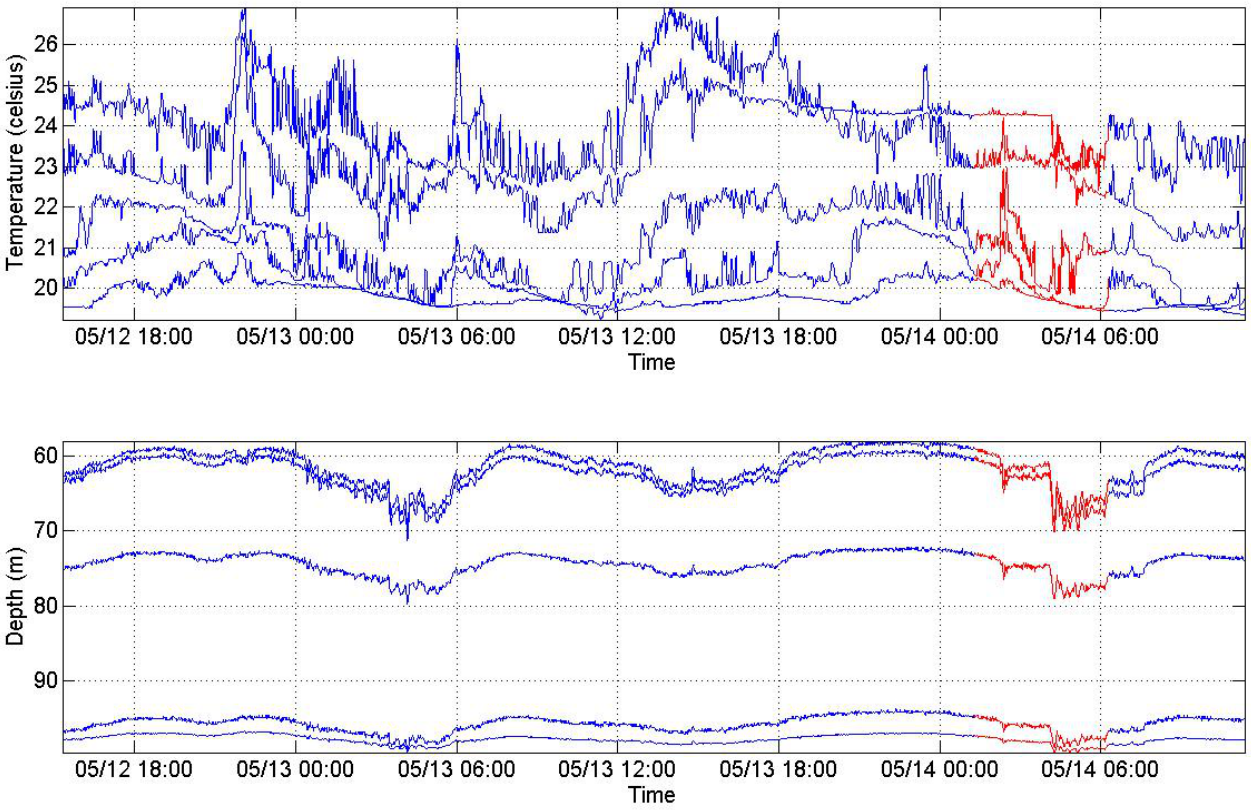

Figure 22 Depth and Temperature record for M-120

2. 2020 Intensive Main Experiment

The intensive main experiment was conducted in the NE SCS and Taiwan Strait in October, 2020 with the RV Legend ship, in which Dr.Ying-Tsong Lin, John Kemp, and Peter Koski from WHOI participated. Owing to the rough sea due to monsoon, the designated experimental area was modified and moved toward Taiwan. For the experiment, four moorings of acoustic and oceanographic gears were deployed along the shelf break from Taiwan Bank to the NE SCS. Figure 23 shows the deployed site of the four moorings and the cruise tracking. The sites M1 and M2 are on the slope. M4 and M3 are on the plateau and canyon, respectively. M1 and M4 are the source moorings with a low-frequency acoustic transmitter system. Further, four moorings were mounted onto the SHRU system, containing an array of four hydrophones from WHOI and the single channel recorder from NSYSU. Figure 24 (a) shows the picture of the receiver mooring deployment.

For acoustic transmission experiment, towed and moored sources (M1 and M4) from NSYSU and WHOI, respectively, were deployed to transmit the midfrequency and low-frequency signals along a designed 40 km track. These signals were received by the moored and towed receivers. For the collection of oceanographic data, multiple T/P sensors were mounted onto the moorings to monitor the temperature profiles. Further, the CTD data of three mooring sites, M1, M3, and M4, were collected for the sound speed profile. In addition, a chirp sonar survey was conducted to collect geoacoustic data. Figure 24 (b) shows the picture of the towed source system deployment.

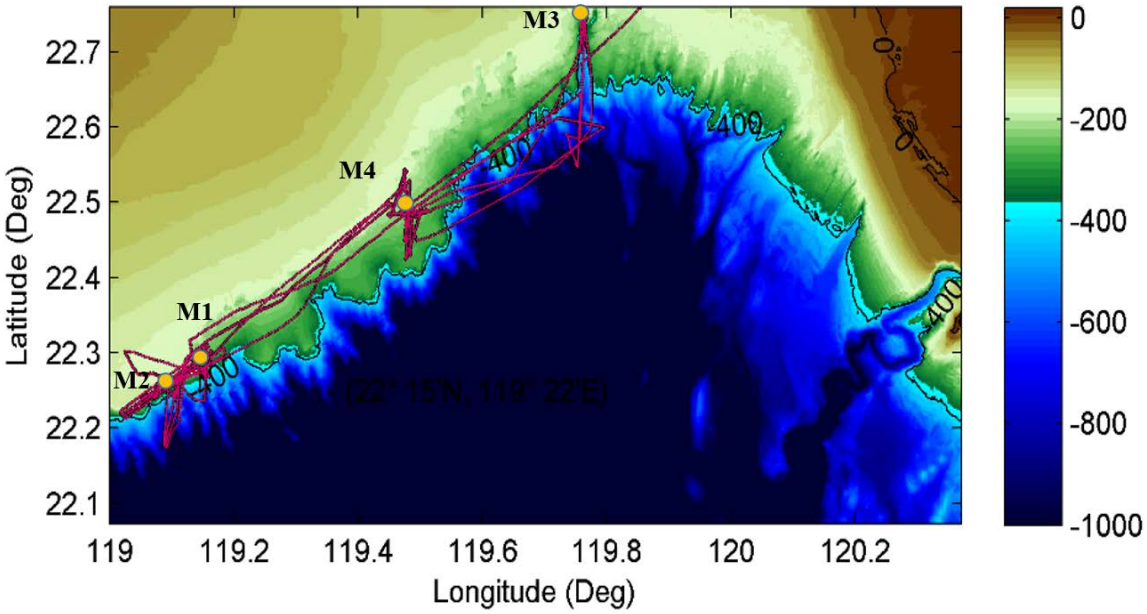

Figure 23 Four moorings deployed site and the complete cruise tracking.

(a) (b)

Figure 24 Pictures of (a) the deployment of receiver mooring from WHOI and (b) deplyment of the towed source from NSYSU.

2.1. The Ship Time and MBES Survey

In September, 2020, before conducting the acoustic experiment with RV Legend, a multibeam survey cruise was conducted with the new RV OR3 ship for aquiring the geomorphology data of the

experimental area, as shown in Figure 25. During the RV Legend cruise, multibeam survey was also conducted around (1) the mooring site M1 and M2 (Figure 26) and (2) the mooring sites M3 and M4 (Figure 27). Meanwhile, to advance the resolution of the data, a set of bathymetric data were purchased from ocean data bank of the Ministry of Science and Technology, Taiwan. Figures 28 and 29 show the integrated bathymetry data of the multibeam data and the database of the plateau and canyon areas.

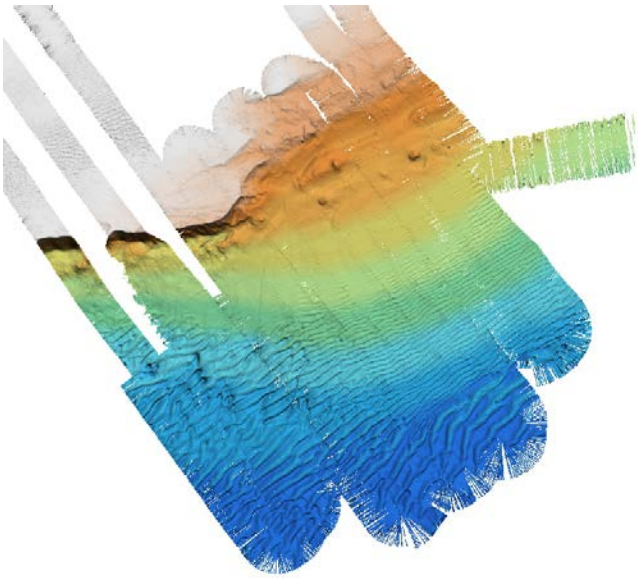

Figure 25 Multibeam echo sounding survey of shelf break area in the NE SCS with the RV New OR3.

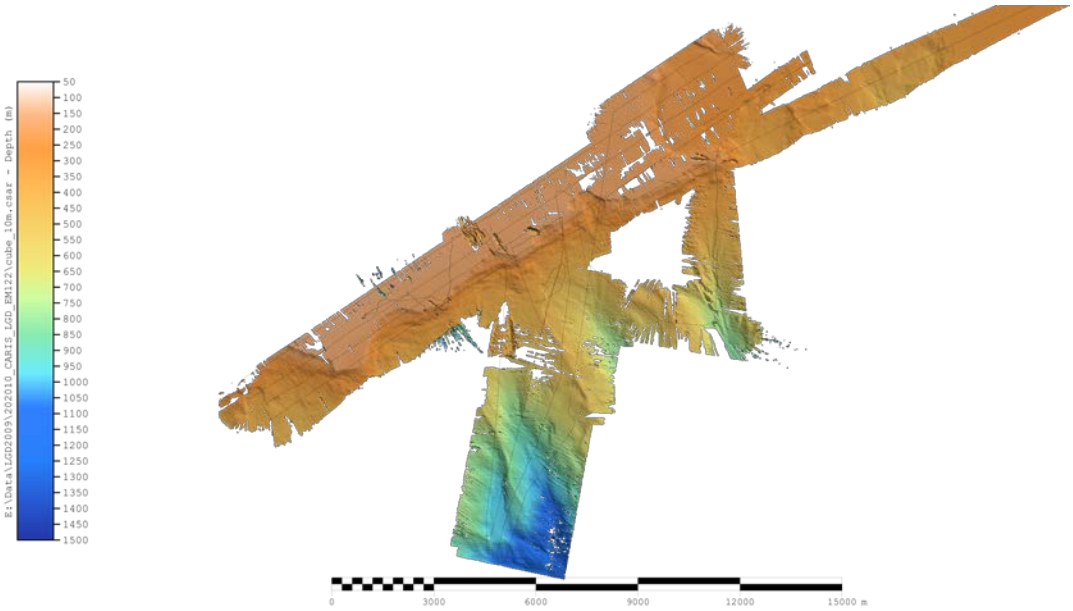

Figure 26 Multibeam echo sounding survey of canyon area and obtained data collected by the RV Legend around sites M1 and M2.

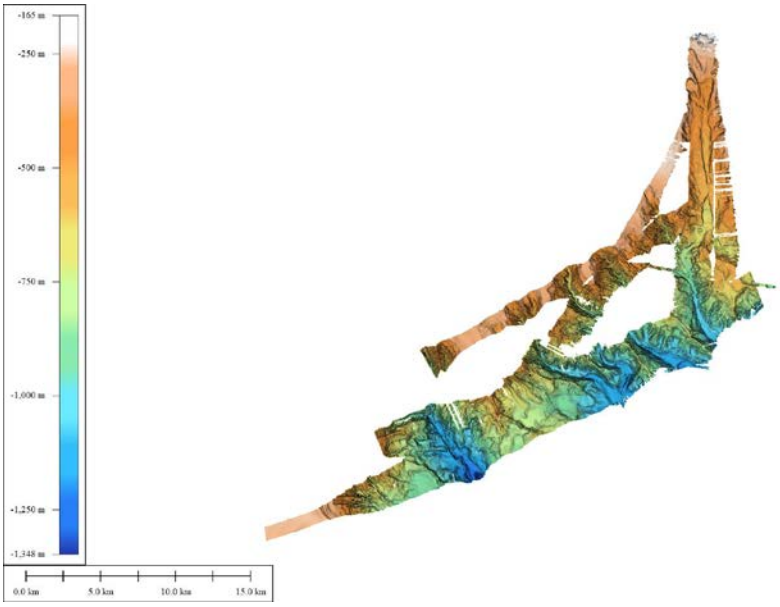

Figure 27 Multibeam echo sounding survey of canyon area and obtained data collected by the RV Legend around sites M3 and M4.

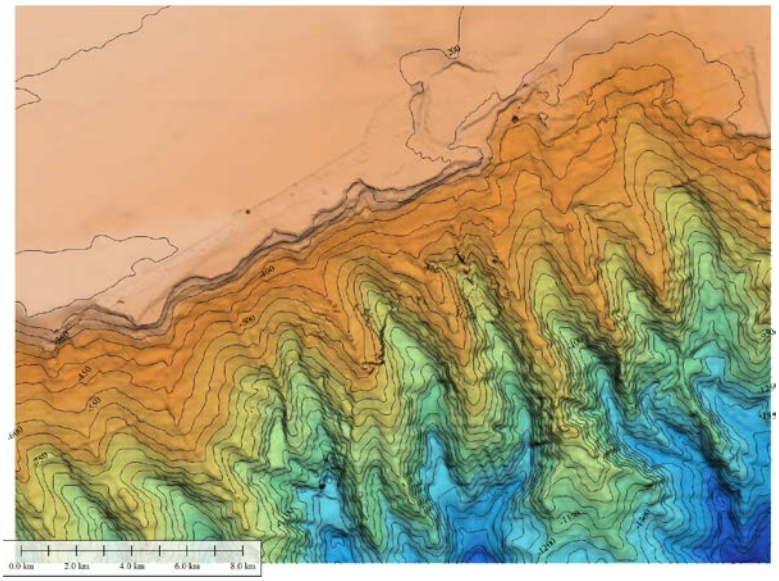

Figure 28 Combination of the multibeam echo sounding survey data and bathymetric database.

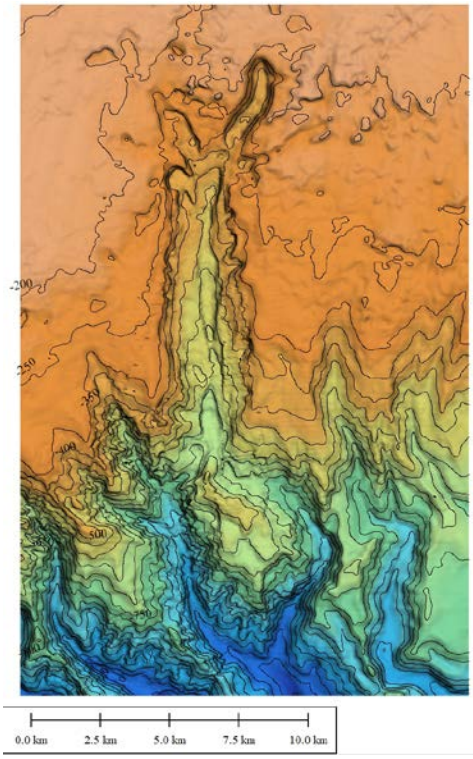

Figure 29 Combination of the multibeam echo sounding survey data and bathymetric database.

2.2. Acoustic Propagation Data Results

Numerous data were collected in the intensive main experiment. The prelimenary data analysis result for an acoustic track along the edge of shelf break is presented here as an example. A main track for acoustic propagation experiment was defined from site M2 to M4. The tow-source tracking line is shown in Figure 30. Figure 31 shows a segment midfrequency (3–7 kHz) acoustic data that have been recorded by the receiver at M1.

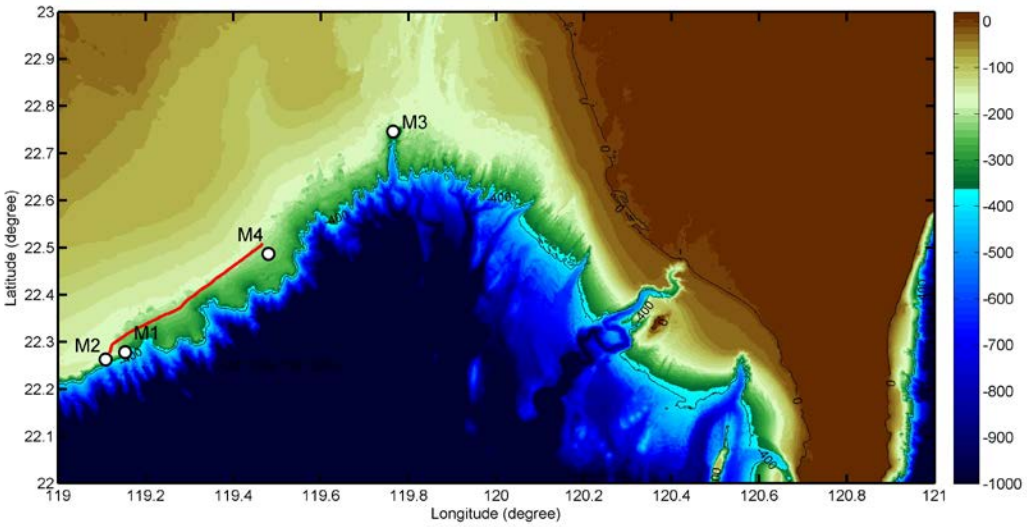

Figure 30 Towed track (M2-M4) of acoustic propagation experiment

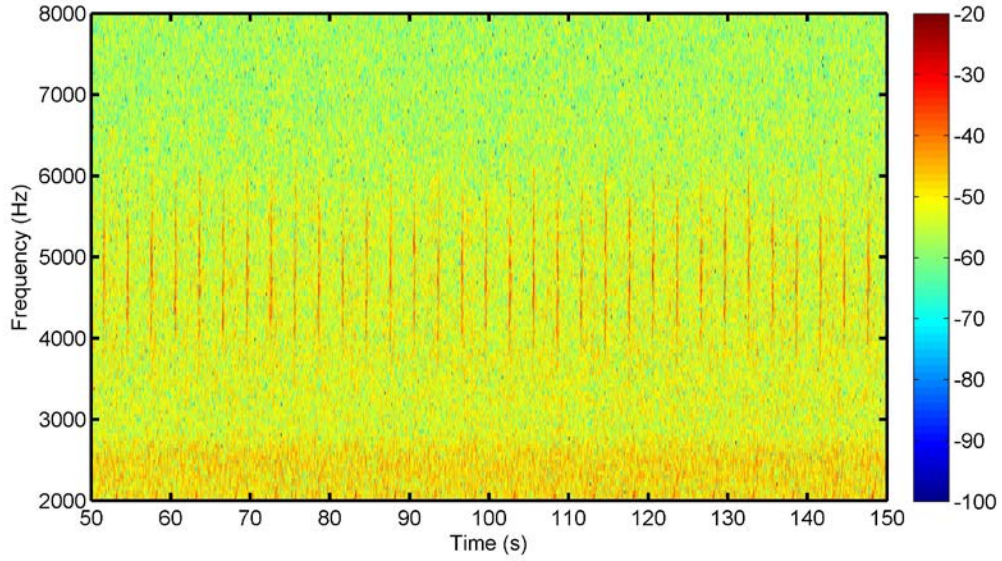

Figure 31 A segment of received midfrequency spectrumgram at M1 for towed track (M2-M4) of acoustic propagation experiment

Another example of the prelimenary data analysis result is the towed survey track around M4 site. Figure 32 shows the towed track around M4, and Figures 33 and 34 show repectively the received spectrugram and impulse responses at M4 site. Data analysis and modeling works will be continued to study the acoustic effects induced by the environmental foactors.

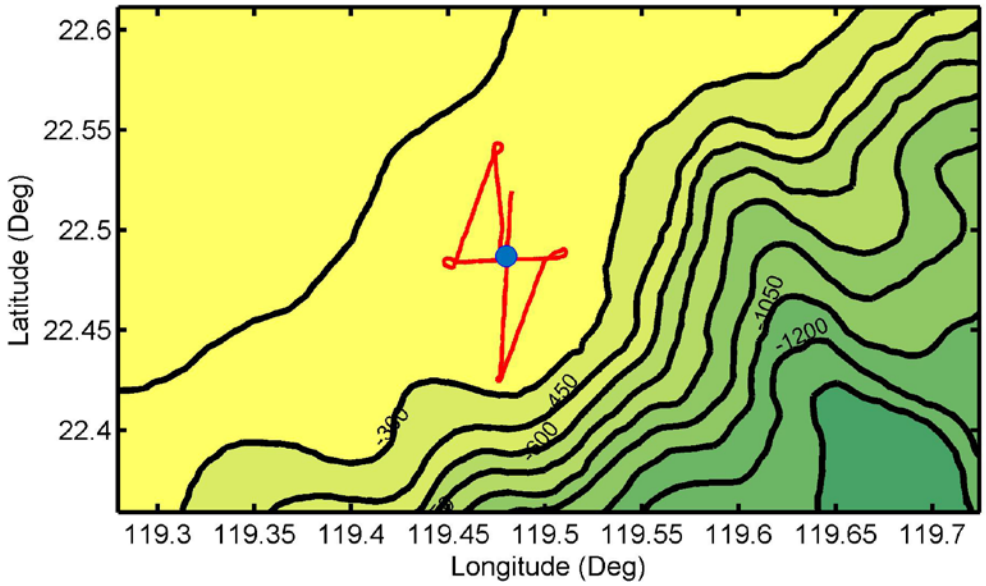

Figure 32 Midfrequency (3–7 kHz) acoustic propagation data along M2–M4 track.

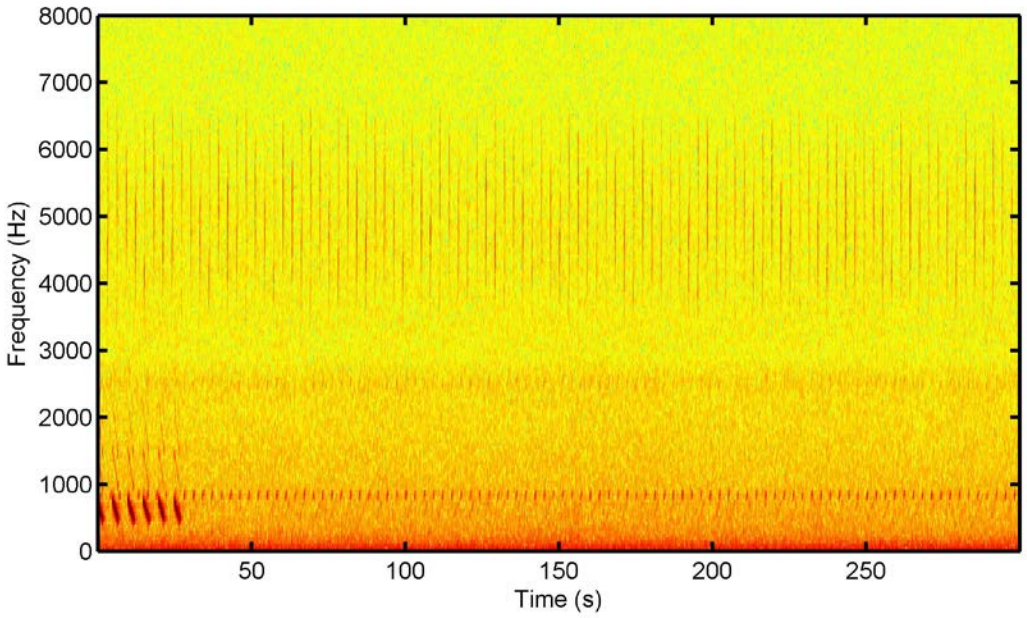

Figure 33 A segment of received midfrequency spectrumgram at M4 for the survey track around M4

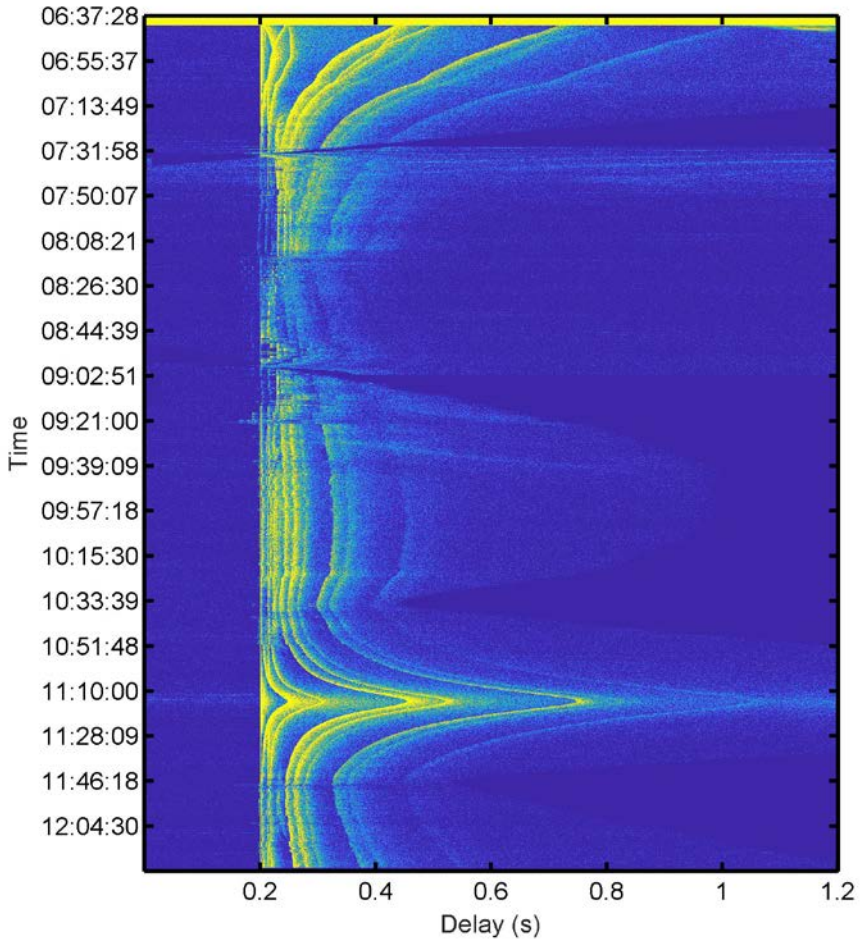

Figure 34 Midfrequency (3–7 kHz) acoustic propagation data at M4 site for the survey track around M4.

2.3. Oceanographic Data

The CTD data three of four moorings (M1, M2 and M3) were collected and shown in Figure 35. Also, plenty numerous temperature and pressure sensors were mounted onto the acoustic moorings to capture the oceanographic features conveyed by the acoustic tracks.

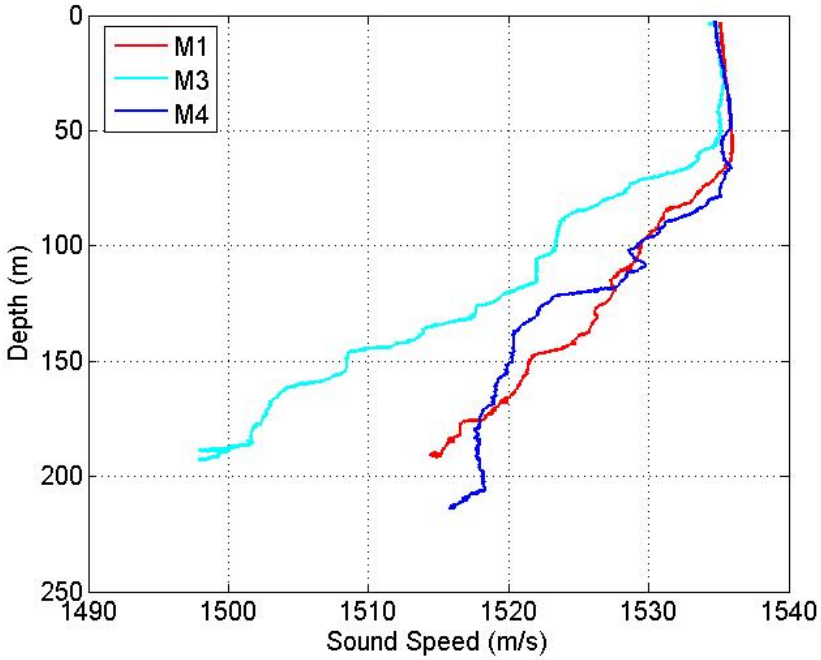

Figure 35 Sound speed profile of three mooring sites.

IMPACT/APPLICATIONS

The acoustic propagation assessment in the pilot experiment is significant and valuable for the acoustic transect spanning across the subaqueous sand dune bedforms, slope, shelf break, and shelf. Large-amplitude internal tides/waves passed along the acoustic path during the experiment. Therefore, the midfrequency and low-frequency acoustic data collected can be used to study the multifactor coupling effects in the NE SCS. In addition, the MBES data obtained in FY19 and FY20 can help in the study of the characteristics and changes in the subaqueous sand dune bedforms and can also be applied in the acoustic modeling studies.

With respect to the bilateral collaboration and the experimental logistics, the pilot experiment facilitated a smooth process and collaboration between NSYSU and WHOI in both years. Further, we have initiated discussions regarding the experimental and logistical plan for FY21 based on the experience FY19 and FY20.

Several acoustic systems were developed by the NSYSU for the acoustic survey of the pilot experiment, including the midfrequency autonomous source, four-channel acoustic self-recorder, and the low-frequency resonant tube. The relevance of this work lies in the stregthening of the experimentation and instrumentation capabilities of Taiwan that is definitely beneficial for future collaboration and further experimentation.

RELATED PROJECTS

This research was supported by the several projects funded by the Ministry of Science and Technology of Taiwan: MOST 108-2623-E-110-001 –D, MOST 108-2623-E-110-002 –D, and MOST 108-2623-E-002 -006 -D.

REFERENCES

Chiu, C.S., Ramp, S.R., Miller, C.W., Lynch, J.F., Duda, T.F., and Tang, T.Y., 2004, “Acoustic intensity fluctuations induced by South China Sea internal tides and solitons,” IEEE J. Ocean. Eng., 29, pp. 1249–1263.

Chiu, L.Y.S., Reeder, D.B., Chang, Y.-Y., Chen, C.-F., Chiu, C.S., and Lynch, J.F., 2013, “Enhanced acoustic mode coupling resulting from an internal solitary wave approaching the shelfbreak in the South China Sea,” J. Acoust. Soc. Am., 133, pp. 1306–1319.

Chiu, L.Y.S., Reeder, D.B., 2013, “Acoustic mode coupling due to subaqueous sand dunes in the South China Sea,” J. Acoust. Soc. Amer., 134, pp. EL198–EL204.

Duda, T.F., Lynch, J.F., Newhall, A.E., Wu, L., and Chiu, C.-S., 2004, “Fluctuation of 400 Hz sound intensity in the 2001 ASIAEX South China Sea experiment,” IEEE J. Ocean. Eng. 29, pp. 1264–1279.

Miller, C.W., Stone, M., Chiu, C.-S., and Ramp, S. R., 2006, Preliminary results from the Windy Island Soliton Experiment (WISE) Acoustics Moorings, Technical Report NPS-OC-06-OXX, Naval Postgraduate School.

Miller, C.W., Reeder, D.B., Stone, M., Wyckoff, K., 2007, Preliminary results from the Non-Linear Internal Wave Initiative (NLIWI) Acoustics Cruise, Technical Report NPS-OC-07-OXX, Naval Postgraduate School.

Newhall, A. et al., 2001, Preliminary Acoustic and Oceanographic Observations from the ASIAEX 2001 South China Sea Experiment, Technical Report WHOI-2001-12, Woods Hole Oceanographic Institution.

Reeder, D.B., Ma, B.B., Yang, Y.J., 2011, "Very large subaqueous sand dunes on the upper continental slope in the South China Sea generated by episodic, shoaling deep-water internal solitary waves" Mar. Geol., 279, pp. 1–4, 12–18.

PUBLICATIONS

1. Peer refereed papers

2020 Chiu, L.*, Chang, A., Chen, H.H., Wang C.H., and Lou, J.Y., "Error analysis on normal incidence reflectivity measurement and geoacoustic inversion of ocean surficial sediment," Continental Shelf Research, vol. 201, pp. 104123.

2019 Chang, A., Chiu, L.*, Mok, M.H.K., Soong, K., and Huang, W.J., "Experimental observations of diurnal acoustic propagation effects in seagrass meadows on the Dongsha Atoll," J. Acoust. Soc. Am., vol. 146, pp. EL279–EL285.

EQUIPMENT

No equipment was purchased in this project.